Received March 22, 2019, accepted March 30, 2019, date of publication April 4, 2019, date of current version April 19, 2019.

Digital Object Identifier 10.1109/ACCESS.2019.2909278

Electromagnetic Characteristics of Permanent Magnet Linear Generator (PMLG) Applied to Free-Piston Engine (FPE)

YONGMING XU[1], DIYUAN ZHAO[1], YAODONG WANG[2], AND MENGMENG AI[1]

[1]School of Electrical and Electronic Engineering, Harbin University of Science and Technology, Harbin 150080, China
[2]Sir Joseph Swan Centre for Energy Research, Newcastle University, Newcastle upon Tyne NE1 7RU, U.K.

Corresponding author: Yongming Xu (xuyongming@hrbust.edu.cn)

ABSTRACT The electromagnetic characteristics of the permanent magnet linear generator (PMLG), which is the key components of the free-piston engine (FPE), are studied in this paper. First of all, the velocity, displacement, and output voltage of the flat-type linear generator used in the experimental platform in the half-motion cycle are simulated by the model of 3D electromagnetic field and verified by experiment, and the relation curves of the output voltage to running velocity are found. Then, the PMLG is re-designed as a tubular type with two different structures of the permanent magnet on the steel backing of the mover: rectangular and the I-shaped. Third, the new PMLGs are modeled, and the models are used to do a simulation to investigate the influence of the structure of permanent magnet on the electromagnetic characteristics under no-load and load conditions. It is found that the fundamental wave amplitude of the flux density in the air gap of I-shaped PMLG is 0.93 T, greater than the rectangular one (0.87 T), and the proportion of the fundamental wave is higher. The waveform of the no-load induced electromotive force of the I-shaped PMLG is much better than that of the rectangular one, and the voltage total harmonic distortion (VTHD) is only 3.05%. The detent force analysis shows that the permanent magnet shape has a great influence on the detent force, and the peak value of detent force between I-shaped and rectangular PMLGs is significantly decreased from 25.4 to 7.75N. Moreover, the relation of the generator output power–velocity and efficiency–velocity under different loads is found. When the load is constant, with the velocity increases, the difference of output power between the I-shaped and rectangular structures becomes bigger. The optimum range of running velocity of the generator with the higher efficiency under different loads is presented. In conclusion, the I-shaped structure of the permanent magnet is a better choice for FPE.

INDEX TERMS Free-piston engine, optimum range of running velocity, permanent magnet linear generator, structures of permanent magnet structure, voltage total harmonic distortion.

I. INTRODUCTION

With the rapid development of electric vehicles, free-piston engine (FPE) system has become a research hotspot because of its simple structure and high efficiency of generator [1], [2]. Currently, there are two main ways to drive a FPE, compressed air and internal combustion [3].

Xiaochen *et al.* [4] presented a free-piston expander linear generator (FPELG) for small scale organic Rankine cycle (ORC). Based on experiment configuration, performance investigation and efficiency analysis on FPELG were carried out. Experiment results showed that intake pressure and external load resistance have great influence on actual stroke, velocity and exhaust temperature. The exhaust pressure was hardly relevant to intake pressure and operation frequency. Xu [5] studied the power generation system of a free-piston internal combustion, the influence of injection starting point, curve of fuel injection and orifice on the formation and combustion process of cylinder mixture was simulated. Wang *et al.* [6] carried out an experimental study on a FPE driven by compressed air, and the relationship between output voltage, motion frequency, conversion efficiency and pressure were also presented. Yonghong *et al.* [7] developed a new FPELG prototype for small scale ORC waste heat recovery system. The in-cylinder pressure, motion characteristics and output performance of the FPELG with different

The associate editor coordinating the review of this manuscript and approving it for publication was Mehmet Alper Uslu.

valve timings were investigated. Zhang *et al.* [8] studied the motion characteristics of a free-piston expander (FPEx) linear generator prototype on the compressed air test platform. It was found that increasing the intake pressure and optimizing the valve timing can significantly improve the output power of the linear generator. Boru *et al.* [9] reviewed and compared the friction mechanisms of free-piston engine and crankshaft engine (CSE) of similar size. It was found that the FPE didn't show advantage on piston ring friction force over the CSE, and the frictional loss from the piston ring was even higher. While the elimination of the crankshaft system reduced the frictional loss of the FPE, and the total friction loss of the FPE was nearly half of the CSE. Preetham and Weiss [10] and Champagne and Weiss [11] tested the operation characteristics of a small scale FPEx. They also performed initial experiment on the small scale FPEx, and the result indicated that higher viscosity lubricants sealed was more effective in static environments than lower viscosity ones. Wu *et al.* [12] investigated a wide range of structure and operating parameters of a FPE including the intake port radial angle, intake port height and operating frequency. The highest scavenging efficiency was 11% higher than that of the original design. Gao *et al.* [13] investigated wave energy converters with direct-driven linear generators. The performance of the system was shown to be sensitive to the load resistance, the wave height, and the spring constant. Chenheng *et al.* [14] performed an experiment to analyze the ignition characteristics of a compression ignited diesel free-piston engine alternator (FPEA). Meanwhile, the effects of injection position and starting force on the ignition were also investigated.

Wang and Howe [15], Chen *et al.* [16], and Wang *et al.* [17] analyzed the electromagnetic characteristic of permanent magnet linear generator (PMLG), and improved generator performance by changing structural parameters such as ratio of stator and mover to outer diameter. Lim *et al.* [18] and Hlaing and Myint [19] studied the influence of pitch on generator detent force, on the basis of the electromagnetic calculation of the piston type tubular linear generator. They found that reasonable adjustment distance can reduce the cogging force and improve generator performance results. Zheng *et al.* [20] studied the electromagnetic performance of axial flux PMLG, they found that the thrust fluctuation of the generator can be reduced by changing the shape of the tooth at both ends of the stator. Chen *et al.* [21] analyzed the 3D magnetic field of the free-piston permanent magnet DC linear generator. They found that the detent force fluctuation was weakened by properly changing the axial length of the permanent magnet. Li *et al.* [22] and Zheng *et al.* [23] optimized the efficiency and power density of a tubular PMLG by changing the permanent magnet material, the number of poles and the length of the actuator. Jalal *et al.* [24] analyzed the electromagnetic of three types of tubular linear generators with radial, quasi Halbach and axial magnetization. The results from their study showed that the magnetic energy utilization and power density of the axial magnetizer were high.

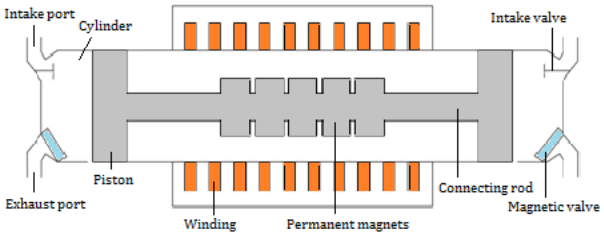

FIGURE 1. Permanent magnet linear generator applied to FPE system.

Sui *et al.* [25] optimized the single-phase tubular PMLG by using the hybrid Halbach / axial magnetization permanent magnet array, and the power density was improved. Zheng *et al.* [26] optimized the design of the PMLG by adjusting the axial and radial length ratio of permanent magnet, the voltage waveform was improved. These studies mainly focus on the design and optimization of the linear generators only.

Few studies had been done on the performance and characteristics of linear generators when they are coupled with FPE/FPEx. It is therefore necessary to carry out study in the area. The aim of this study is to investigate the electromagnetic characteristic of a PMLG coupled with a FPE driven by compressed air. The experimental test rig for the FPE system that built in the previous period is utilized to study the operation and output characteristics of the flat linear generator; computational model is set up and verified by the experimental results. The validated models are then used to study the electromagnetic characteristics of the tubular linear generator with the structure of I-shaped permanent magnet coupled with the FPE system.

II. EXPERIMENTAL COMPARISON AND ANALYSIS OF A FLAT PMLG

A. THE SYSTEM OF FPE WITH PMLG

The reciprocating motion of the free-piston linear generator assembly is a nonlinear dynamic system, which is more complex than other systems [27], [28]. The permanent magnet linear generator (PMLG) applied to free-piston Engine (FPE) is shown in Fig.1.

The system is composed of a PMLG, 2 pistons, a connecting rod, 2 air cylinders and other auxiliary components. The gas in the left and right cylinders expands alternately to drive the reciprocating motion of the pistons, which can drive the reciprocating motion of the mover of the linear generator, and it can make the stator winding cut across the magnetic flux and induce the electromotive force (EMF) to complete the energy conversion process from mechanical work to electrical power.

B. EXPERIMENT TEST RIG

The experiment test rig of FPE with PMLG system is shown in Fig. 2. Two free-pistons and a flat PMLG are fixed on the same connecting rod, and the motion of FPE is controlled by a control unit supported by a data acquisition unit with sensors. The pressure, displacement and output voltage of the

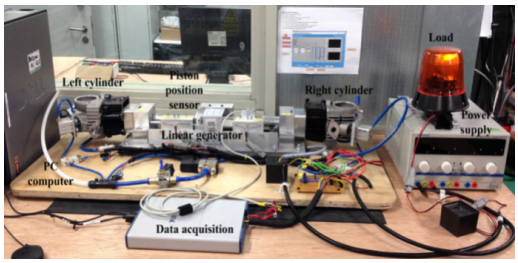

FIGURE 2. The experiment test rig of FPE with PMLG system.

TABLE 1. The main parameters flat permanent magnet linear generator.

Parameters	Value
Power/kW	1
Stator length/mm	300
Stator width/mm	190
Mover length/mm	200
Mover width/mm	180
Pole number	10
Air gap width/mm	1
Permanent magnet material	NdFe30

system are measured and collected by the sensors and the data acquisition unit. The control unit controls the movement of the whole system of FPE and PMLG.

C. FLAT PMLG AND MODEL SET-UP

The main parameters of the flat PMLG in the experimental platform are shown in TABLE 1.

The transient magnetic field of flat PMLG prototype is modeled by Ansoft software. The control equations of transient magnetic field are:

$$\begin{cases} \nabla \times \boldsymbol{H} = \boldsymbol{J}_{\mathrm{s}} + \boldsymbol{J}_{\sigma} \\ \nabla \times \boldsymbol{E} = -\dfrac{\partial \boldsymbol{B}}{\partial t} \\ \nabla \cdot \boldsymbol{B} = 0 \\ \boldsymbol{J}_{\sigma} = \sigma \boldsymbol{E} \\ \nabla \cdot \boldsymbol{J}_{\sigma} = 0 \\ \boldsymbol{B} = \mu \boldsymbol{H} \end{cases} \tag{1}$$

where $\boldsymbol{B}$ is vector of magnetic induction intensity (flux density), $\boldsymbol{H}$ is vector of magnetic field intensity, $\boldsymbol{E}$ is vector of electric field intensity, $\boldsymbol{D}$ is vector of electric displacement, ρ is volume density of charge, $\boldsymbol{J}_{\mathrm{s}}$ is conduction current density, $\boldsymbol{J}_{\sigma}$ is eddy current density, ε is dielectric constant, σ is electric conductivity, μ is magnetic permeability.

The three-dimensional model of flat PMLG prototype is shown in Fig. 3.

D. EXPERIMENT VALIDATION

The movement process of the flat PMLG is simulated and the results are compared with the experimental results from

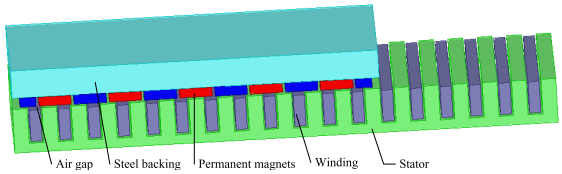

FIGURE 3. The three-dimensional model of flat PMLG.

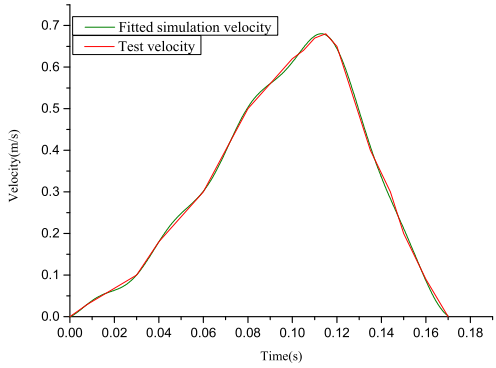

FIGURE 4. The velocity-time curve of generator mover.

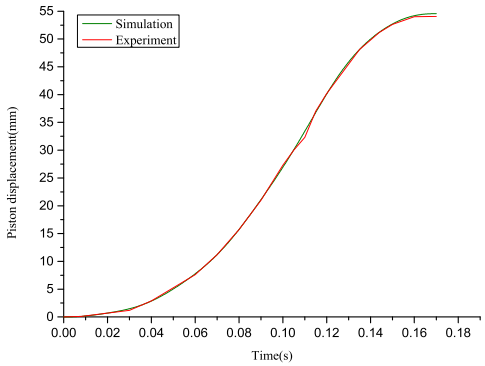

FIGURE 5. The displacement-time curve of generator mover.

the tests. The velocity of the pistons and generator mover in the reciprocating cycles is shown in Fig.4. As the movement of the FPE and PMLG is reciprocating process, the forward and backward movements are the same but in different direction. So the following results in figures are shown in a half period.

Fig.4 shows the variation curve of velocity-time of the generator mover (and the free-piston). It can be seen from Fig.4 that the peak velocity from simulation is 0.68m/s, compared to that experimental result (0.65m/s) at the time of 0.11s-0.12s. The relative error between the two is 4.62%.

The displacement-time curve of generator mover is shown in Fig.5. It can be seen from Fig. 5 that the displacement of generator mover is nearly the same as the experimental result. The displacement of the generator is 54.56mm from simulation, compared to that 53mm from experiment, the relative error between the two displacements caused by the fitted velocity-time curve is 2.94%.

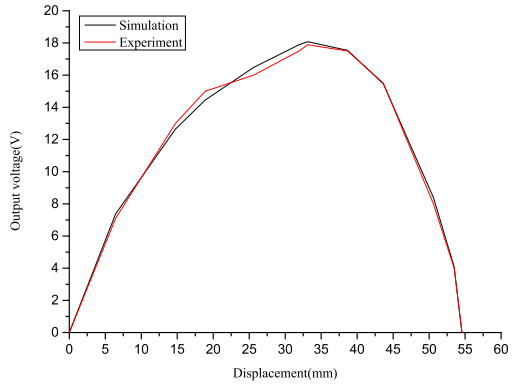

FIGURE 6. The output voltage-displacement curve of the generator.

The output voltage-displacement curve of the generator is shown in Fig.6. It can be seen from Fig.6 that the peak voltage from the simulation is 18.08V, 0.19V larger than that from experimental (17.89V). The maximum voltage difference between simulation and experiment is 0.4V at the displacement of 25mm-30mm, and the maximum relative error is 2.5%. In summary, the maximum relative error between simulation and experiment is less than 5% which can proves that the simulation model and method of PMLG coupled with FPE are accurate and feasible. In the following sections, the method of modeling and simulation will be applied to simulate tubular PMLG re-designed for FPE.

III. ELECTROMAGNETIC DESIGN AND PERFORMANCE ANALYSIS OF A TUBULAR PMLG

The PMLG used in the experimental test rig in Fig.2 is a flat one. It is found that the power generated from it is low. In contrast, tubular PMLG has its advantage over the flat one: there is no transverse margin effect and radial one-sided magnetic pull [29]. Therefore, a tubular PMLG is designed and modeled to study its electromagnetic characteristics and the influence of FPE system on the performance.

Where η: assumed value of the generator efficiency; cosφ: assumed value of the power factor; F: assumed value of the starting thrust; ε: assumed value of the electric potential coefficient; η': calculated value of the efficiency; cosφ': calculated value of the power factor; F′: calculated value of the starting thrust; ε': calculated value of the electric potential coefficient; I: Number of iterations; Im: Maximum number of iterations; $\Delta\eta$: the difference between η and η'; Δcosϕ: the difference between cosφ and cosφ'; ΔF: the difference between cosφ and cosφ'; $\Delta\varepsilon$: the difference between ε and ε'.

A 3kW tubular PMLG prototype with 18 stator slots and surface-mount permanent magnet fixed on the movable steel backing of mover is designed. The whole process includes design of stator lamination, design of permanent magnet material, shape and size on steel backing in mover, calculation of resistance and reactance and the performance calculation of PMLG. A detailed design flow scheme is shown in Fig.7. The basic parameter of the tubular PMLG is show in TABLE 2.

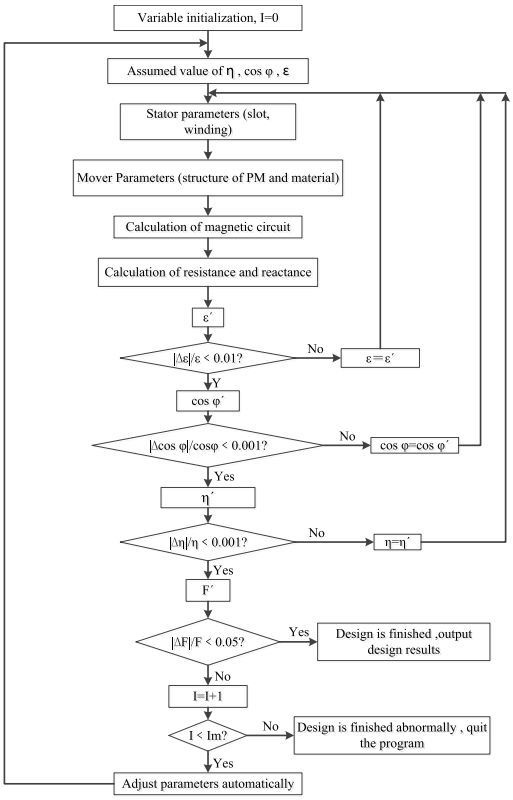

FIGURE 7. The design flow scheme of tubular PMLG prototype.

In order to investigate the influence of structure of permanent magnet on the electromagnetic characteristics of the tubular PMLG, two different structures of permanent magnet in mover are designed. One is rectangular, the other is I-shaped and the material and size of permanent magnet is uniform. That is to say, the two movers are the same except the structures of permanent magnet. The mover of tubular generator can be replaced by another.

TABLE 2. The basic parameters of tubular PMLG.

Parameters	Value
Power/kW	3
Stator length/mm	296
Outer diameter of stator/mm	122
Inner diameter of stator/mm	74
Slot depth of stator/mm	19
Slot pitch of stator /mm	16
Tooth width of stator /mm	8
Pole pitch of permanent magnet /mm	19.2
Radial height of permanent magnet /mm	5
Width of air gap /mm	1
Number of coil turns per slot	21

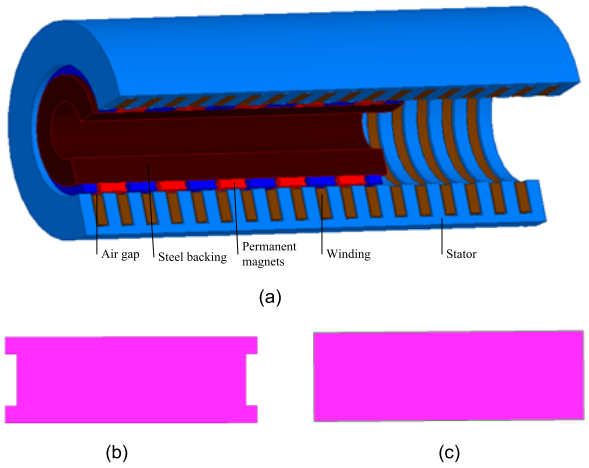

FIGURE 8. The 3D model of tubular PMLG and two permanent magnet structures. (a) 3D model of tubular PMLG. (b) I-shaped structure. (c) Rectangular structure.

The 3D model and two permanent magnet structures are shown in Fig.8. Fig.8 shows the 3D model of the tubular PMLG and two structures of permanent magnet: rectangular and the I-shaped structure. Its permanent magnet adopts radial magnetization to improve the flux density in air gap and the efficiency of generator. The armature winding adopts the modular cake structure, as the structure is simple and easy to install.

IV. RESULTS AND DISCUSSION

A. MAGNETIC FIELD ANALYSIS OF TUBULAR PMLG

The transient magnetic field tubular PMLG is modeled by Ansoft software. The control equations of transient magnetic field are shown in equations (1). The results of flux density distribution of the tubular PMLG with rectangular and I-shaped structures under no-load and load condition are shown in Fig.9.

In Fig.9, the flux density of the detection point is selected and compared. The flux density of rectangular PMLG under no-load and load condition are 1.042T and 1.051T separately and the flux density of I-shaped PMLG under no-load and load condition are 1.126T and 1.131T. It can be seen from the results, the flux density under load condition is greater than that under no-load condition for the same structure of permanent magnet due to the armature reaction and no matter any condition, the flux density of I-shaped PMLG is greater than that of rectangular PMLG. It also can be seen from Fig. 9, under no-load condition the maximum value of tooth flux density of rectangular and I-shaped PMLG is 1.626T and 1.721T separately and the maximum value of yoke flux density is 0.663T and 0.679T. Therefore, it is found that the I-shaped PMLG has higher material utilization and can improve the power density by decreasing the effective material consumption.

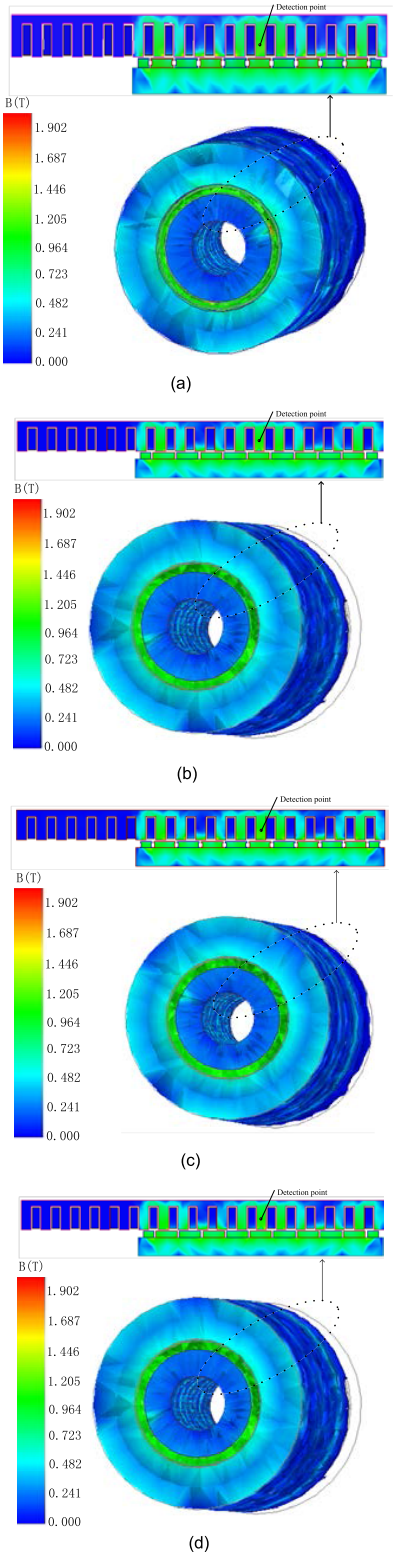

FIGURE 9. The flux density distribution of the tubular PMLG with rectangular and I-shaped structures under no-load and load condition. (a) The flux density distribution of rectangular tubular PMLG under no-load condition. (b) The flux density distribution of I-shaped tubular PMLG under no-load condition. (c) The flux density distribution of rectangular tubular PMLG under load condition (5 Ω). (d) The flux density distribution of I-shaped tubular PMLG under load condition (5 Ω).

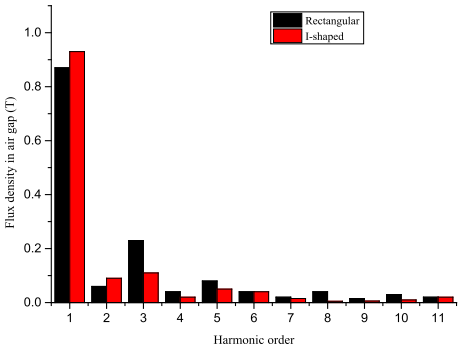

FIGURE 10. Harmonic analysis of the no-load flux density in air gap of the generator with two mover structures.

B. THE FLUX DENSITY IN AIR GAP

The energy conversion of the generator relies on the flux density in air gap; and the magnitude of flux density in air gap determines the power generated by the generator directly. Fig.10 shows the results of the no-load flux density in air gap under a pair of magnetic poles of the tubular linear generator with two mover structures from Fourier harmonic analysis.

It can be seen from Fig.10, the fundamental wave amplitude of I-shaped PMLG is 0.93T, which is 6.9% larger than the fundamental wave amplitude of rectangular one of 0.87T. The proportion of fundamental wave of the I-shaped and the rectangular mover is 77% and 66%, respectively. It means that I-shaped structure can obviously improve the sinusoidal waveform of the flux density in air gap under the no-load condition.

C. NO-LOAD INDUCED ELECTROMOTIVE FORCE

In order to verify the performance of the tubular permanent magnet linear generator designed in this study, the induced electromotive force waveforms of the two kinds of permanent magnet structure generators operate at a velocity of 3m/s are studied and the results are shown in Fig.11.

It can see from Fig.11, the amplitudes of the induced electromotive force of rectangular generator of A, B, C Phase are 48.14V, 48.13V, 47.98V, respectively. In comparison, the amplitudes of the induced electromotive force of I-shaped generator of A, B, C Phase are 47.89, 47.83, 48.64V, respectively. The magnitudes of the induced electromotive force of two structures are approximately equal. However, the shape and symmetry of induced electromotive force waveform of the I-shaped generator is obviously better than that of rectangular generator. Due to the symmetry of the three-phase induced electromotive force, the C phase waveform is the only one that Fourier harmonics decomposed, as shown in Fig. 12.

$$\mathrm{VTHD} = \frac{\sqrt{(\mathrm{U}_2^2 + \mathrm{U}_3^2 + \cdots + \mathrm{U}_\mathrm{n}^2)} \times 100\%}{\mathrm{U}_1} \qquad (2)$$

where the U_n is root mean square (rms) of the nth harmonic voltage, U_1 is the rms of fundamental waveform voltage.

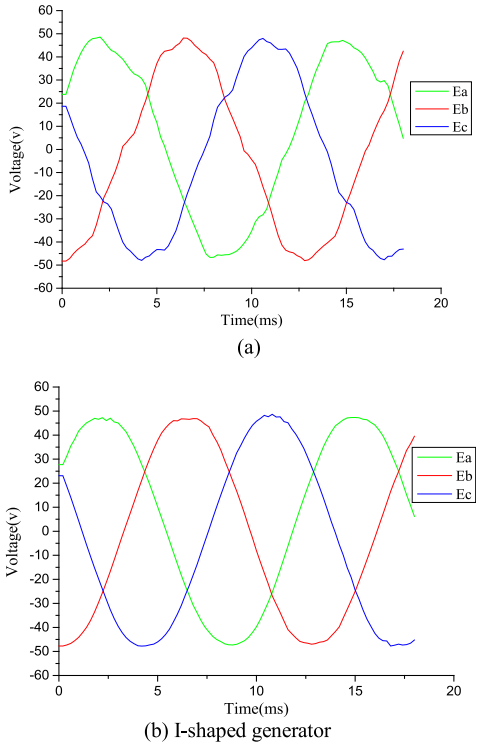

FIGURE 11. The no-load induced electromotive force waveform at 3m/s. (a) Rectangular generator. (b) I-shaped generator.

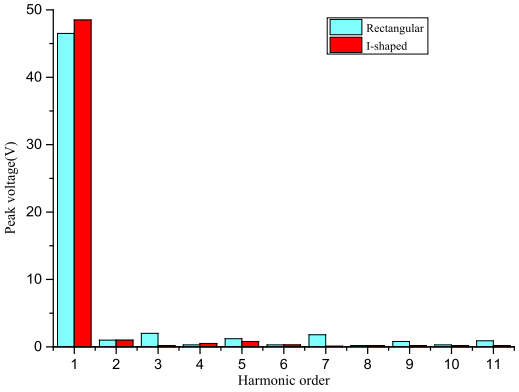

FIGURE 12. Harmonic analysis of C-phase induced electromotive force.

It can be seen from Fig.12 that the peak value of electromotive force fundamental wave of I-shaped PMLG is 48.5V, which is 2V larger than that of the rectangular one 46.5V. The voltage total harmonic distortion (VTHD) of the I-shaped PMLG calculated by equation (2) is 3.05%, while the rectangular PMLG up to 7.27%. Compared to the rectangular generator, the I-shaped generator obviously improves the output voltage waveform.

D. ANALYSIS OF DETENT FORCE

Detent force is one of the inherent characteristics of PMLG and is mainly composed of two parts. One is the cogging force caused by the interaction between the permanent magnet

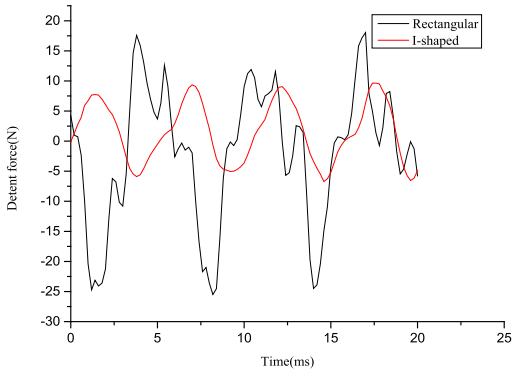

FIGURE 13. The detent force of tubular PMLG with two different mover structures.

and the tooth and slot of the stator, another is the force generated by the margin effect. When the detent force is large, it will cause the larger fluctuation of electromagnetic force of generator, resulting in noise, even resonance at low frequency, which will have great influence on the performance of the PMLG. For a FPE system, the detent force will hinder the movement of the mover and affect the efficiency of the system. Furthermore, the larger detent force will affect the electromagnetic force waveform, and then influence the induced electromotive force waveform, so it is necessary to reduce the detent force as much as possible.

The detent force of tubular PMLG with two different mover structures is shown in Fig.13. It can be seen from Fig.13 that the peak value of detent force of rectangular permanent magnet mover is 25.4N, the peak value of detent force of I-shaped permanent magnet mover is 7.75N, and the detent force is decreased by 17.65N. It can be seen that the magnitude of the detent force is related to the shape of permanent magnet. Under the same condition, the detent force of the I-shaped PMLG is significantly reduced, which is more suitable for the FPE.

E. OUTPUT POWER AND EFFICIENCY OF GENERATOR

When the PMLG is running, the stray loss and additional loss account for a small proportion, which can be ignored. The copper loss of the winding and core loss are the two main losses which influence directly the output power and efficiency of the generator. The copper loss and core loss of rectangular and I-shaped PMLG under different loads (5 Ω, 10Ω and 15Ω) and velocities are shown in TABLE 3 and TABLE 4 separately.

It can be found from TABLE 3 and TABLE 4 that in the same mover structure, the copper loss of the winding is decreased with the increase of loads at a certain of velocity, but the core loss is basically unchanged under the same condition. Under a certain load condition, the copper loss of the winding and the core loss are increased with the increase of velocity of PMLG. But the output power is increased with the increase of velocity which leads to the increase of efficiency. This conclusion is consistent with the trend shown in Fig.14.

TABLE 3. The loss of rectangular PMLG under different loads and velocities.

Velocity(m/s)	copper loss(w)			core loss(w)		
	5Ω	10Ω	15Ω	5Ω	10Ω	15Ω
0.1	0.021	0.005	0.002	0.44	0.44	0.44
0.5	0.54	0.136	0.06	2.22	2.25	2.25
1	2.15	0.54	0.24	4.8	4.8	4.7
1.5	4.8	1.2	0.54	7.4	7.4	7.4
2	8.4	2.15	0.95	10	10.3	10.4
2.5	13	3.3	1.48	13.5	13.6	13.2
3	18	4.75	2.15	16.8	16.8	16.5
3.5	24	6.3	2.8	19.5	19.5	19.5
4	31	8.2	3.7	23.5	23.5	23.5
4.5	38	10.3	4.6	27	27	27.7
5	46	12.6	5.6	31	31.5	32
5.5	55	15	6.8	35	35	36
6	63	17.6	8.1	39	40	40

TABLE 4. The loss of I-shape PMLG under different loads and velocities.

Velocity(m/s)	copper loss(w)			core loss(w)		
	5Ω	10Ω	15Ω	5Ω	10Ω	15Ω
0.1	0.021	0.005	0.004	0.47	0.47	0.48
0.5	0.52	0.128	0.059	2.4	2.3	2.38
1	2.08	0.51	0.234	5	4.8	5
1.5	4.7	1.16	0.53	7.8	7.7	8
2	8.3	2.04	0.93	10.8	10.8	10.9
2.5	12.7	3.2	1.44	14	13.6	14
3	18.2	4.2	2.08	17.6	17.2	17.6
3.5	24.5	6.4	2.8	21	21	21
4	31.5	8.2	3.65	24.9	25	25
4.5	39	10.3	4.6	28.5	29	28.5
5	47	12.6	5.7	32.6	33	32.5
5.5	56.5	15.2	6.9	36.8	37	37
6	65	17.8	8	40	41	41.5

The output power and efficiency of the generator under different loads are calculated by the copper loss of the winding and core loss. The output power- and efficiency-velocity curves of PMLG under different loads (5 Ω, 10Ω and 15Ω) are shown in Fig.14.

It can be seen from Fig.14 (a), when the load is 5Ω and the velocity is 2m/s, the output power of the two generators is 285W (rectangular) and 300W (I-shaped), respectively. The difference is 15W. When the velocity is 4m/s, the output power is 1080 W (rectangular) and 1155 W (I-shaped). The difference is 75W. The output power difference gradually increases. Compared to the rectangular mover generator, the output power of the I-shaped mover generator is higher when run at the same velocity and load. When the load is fixed (e.g. 5 Ω), the output power difference is getting bigger and bigger with the increase of velocity. When the velocity is fixed,

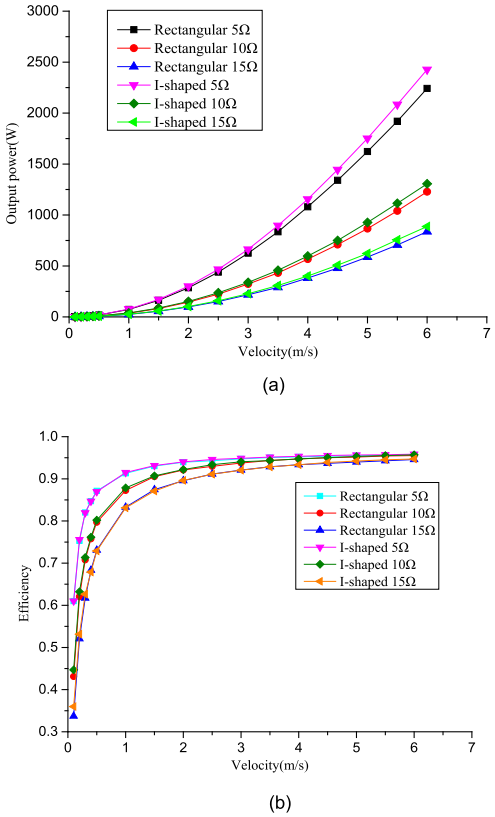

FIGURE 14. The output power- and efficiency-velocity curve of PMLG under different loads. (a) Output power-velocity curve. (b) Efficiency-velocity curve.

the output power difference is getting smaller and smaller with the increase of the load.

It can be seen from Fig.14 (b) that the efficiency of rectangular mover generator and I-shaped one is 91.31% and 91.51% respectively when the load is 5Ω and the velocity is 1m/s, and the efficiency of the I-shaped is slightly increased by 0.2% compared with the rectangular. When the velocity and load are fixed, the efficiency of I-shaped mover generator is higher than that of rectangular one. From the figure, it can also be seen that with the velocity increases, the efficiency of the generator firstly increases sharply, and then it tends to be stable at about 95%. This is due to the fact that as the output power of the generator keeps increasing with the velocity of the generator increases, but the copper loss is also increased, so that the efficiency is not increased. It can be seen that when the velocity is fixed, the efficiency of generator becomes higher with the load decreases. From the above results, it can be seen that the power density and efficiency of I-shaped mover generator are higher than that of rectangular one.

From Fig.14, it can be seen that when the load is 5 Ω and the velocity is 2m/s, the power reaches 300W and the efficiency reaches 94%. When the velocity is 5.5m/s, the power reaches 2 kW and the efficiency reaches 95%, which achieves the maximum efficiency and meets the design requirement. When the load is 10 Ω, the running velocity of generator

TABLE 5. Electromagnetic characteristics comparison of two PMLG.

Electromagnetic characteristics	Structure of permanent magnet	
	Rectangular	I-shaped
No-load flux density of the detection point /T	1.031	1.052
5ohm-load flux density of the detection point /T	1.035	1.085
Fundamental wave amplitude of flux density in air gap /T	0.87	0.93
Peak value of C-phase no-load electromotive force fundamental wave /V	46.5	48.5
Voltage total harmonic distortion /%	7.27	3.05
Peak value of detent force /N	25.4	7.75

can be operated in the range of 2m/s-5.5m/s in order to obtain high efficiency of the generator (> 90%). When the load is 15 Ω, the running velocity of generator can be operated in the range of 4m/s-5.5m/s to obtain high efficiency of the generator (> 90%). Therefore, in order to get higher generator efficiency, the velocity of the generator can be adjusted according to the specific load. For this specific PMLG design, the velocity should not exceed 6m/s and the load should not exceed 15 Ω.

When the velocity is 3m/s, electromagnetic characteristics comparison of rectangular and I-shaped PMLG are shown in Tab.5. It can be found from TABLE 5 that I-shaped PMLG is much better than the rectangular one.

F. THE INFLUENCE OF ENGINE VELOCITY ON THE GENERATOR

In order to find the influence of engine velocity on the performance of the PMLG when driven by the FPE, a further simulation is carried out and the results of no-load induced electromotive force waveform of generator with two different movers are shown in Fig.15.

It can be seen that I-shaped mover generator has better induced electromotive force waveform and less harmonics than that of rectangular one. Compared with constant velocity motion, three-phase induction electromotive force is no longer a symmetrical relationship. The change of the induction electromotive force is directly related to that of the corresponding velocity. The velocity of generator at the two terminals is lower, the amplitude of the induced electromotive force is smaller, while in the middle part of the figure, the velocity is higher and the amplitude of the induction electromotive force is larger. When the velocity reaches the peak value, the induced electromotive force (voltage) also reaches the maximum value 96.3V. This shows that the induction electromotive force is proportional to the velocity.

The output terminal of the generator connects the load of 5 Ω, the instantaneous output power and the instantaneous

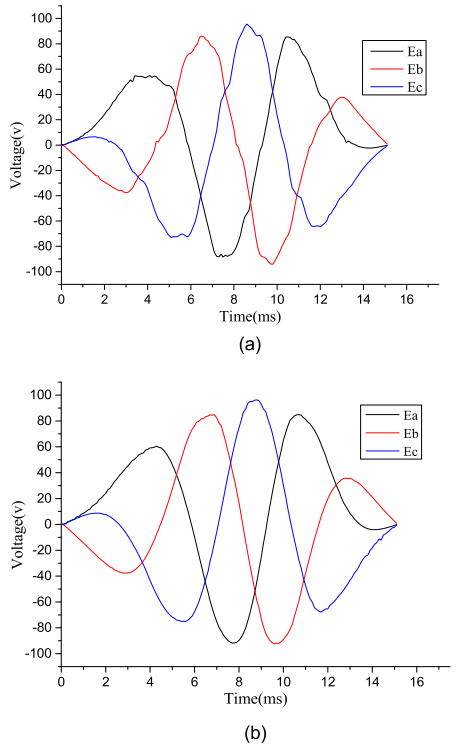

FIGURE 15. The no-load induced electromotive force waveform of generator with two different movers. (a) Rectangular mover. (b) I-shaped mover.

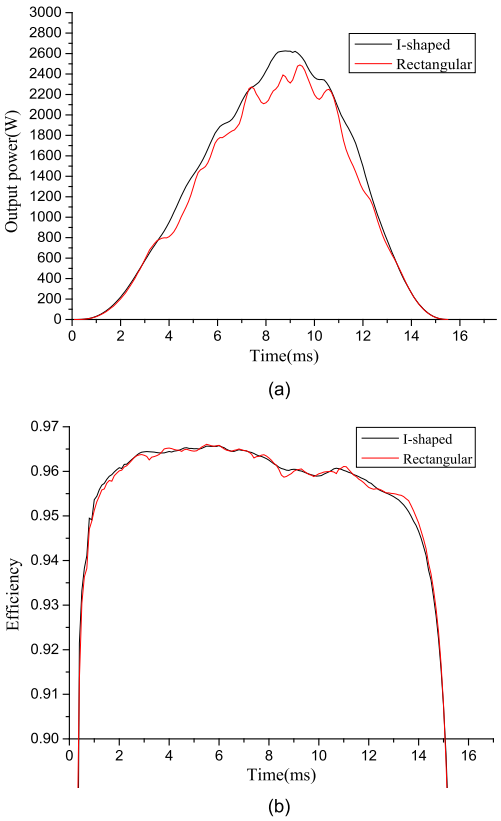

FIGURE 16. The curve of the instantaneous output power and efficiency of generator with two kinds of movers. (a) Instantaneous power. (b) Instantaneous efficiency.

efficiency of generator with two kinds of movers is shown in Fig.16. It can be seen from Fig.16 (a) that the instantaneous output power from the two generators are the same in the lower velocity of both terminals, but the difference is larger at high-velocity in the middle part of the curves. This is because the outputs of voltage and current of the two generators are different, so the power outputs are different. The power of I-shaped permanent magnet generator is 310W higher than that of rectangular one at 9m/s. It can be seen from Fig.16 (b), the overall efficiency of I-shaped permanent magnet generator is slightly higher than that of the rectangular one.

From the above results, it can be seen that, under the FPE system operation condition, the I-shaped permanent magnet generator has better induction electromotive force waveform, higher overall power and efficiency, and more stable than that of the rectangular structure generator.

The relation of output power-velocity of the I-shaped permanent magnet generator is shown in Fig.17. It includes the output power when it is run at constant velocity; the instantaneous output power and the trend line of average instantaneous power when it is run at varied velocity (driven by the FPE).

It can be seen from the in Fig.17 that when the velocity is 3m/s, the output power is 575W during the rising process and the output power is 896W during the decline process. It is known that the instantaneous power in the process of velocity rise is smaller than that of the same velocity in the process of decline. This is because the change rate of the

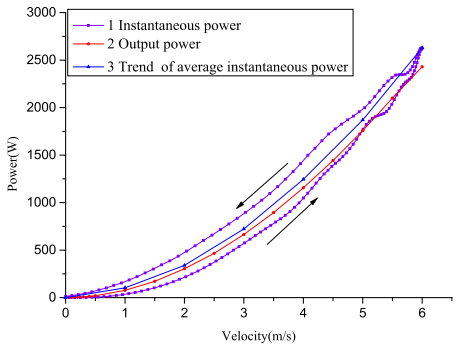

FIGURE 17. The relation of output power-velocity of the I-shaped permanent magnet generator.

flux in the winding increases gradually in the process of rising velocity. The induced current in windings can hinder flux change rate to increases, the increase of electromotive force is suppressed, resulting in smaller instantaneous power output. In the process of deceleration, the effect is opposite. Therefore, the less time the velocity increases to the peak value is, the higher the output power of the generator will be. It can be seen from the curves 2 and 3 in the figure, when the velocity is 1 m/s, the value of curve 2 is 76.8W and the value of curve 3 is 103W, the difference between the two is 26.2W. When the velocity is 5m/s, the value of the curve 2 is 1757.7W and the value of curve 3 is 1870W, the difference between the two is 112.3W. It can be seen that the power difference

between curve 2 and curve 3 increases with the increase of velocity.

V. CONCLUSIONS

In this paper, the operating characteristics and output characteristics of tubular permanent magnet linear generator using I-shaped and rectangular designs are studied based on the experimental results from the flat PMLG. The following conclusions can be drawn:

1) A tubular PMLG which is suitable for the FPE system is designed. The performance of the two permanent magnet structure generators (I-shaped and rectangular) are compared and analyzed. The detent force of the permanent magnet is smaller, the amplitude of the air-gap flux density is larger, the voltage total harmonic distortion is smaller, and the output voltage waveform of generator is improved.
2) The output power and efficiency of the I-shaped PMLG are higher than that of rectangular one. I-shaped PMLG has better induced electromotive force waveform and less harmonic content than that of rectangular PMLG. The overall efficiency of I-shaped PMLG is slightly higher than that of the rectangular structure generator.
3) When driven by the FPE, the induced electromotive force waveform varies with the velocity of the FPE; the I-shaped PMLG has better induced electromotive force waveform and less harmonic content than that of rectangular one; the velocity is higher and the amplitude of the induction electromotive force is larger and the power output is higher. The optimum range of running velocity of the generator with the higher efficiency under different loads is presented.

REFERENCES

[1] S. Schneider and F. Rinderknecht, "A high efficient energy converter with flex fuel potential," in *Proc. Int. Conf. Clean Elect. Power (ICCEP)*, Alghero, Italy, Jun. 2013, pp. 453–460.
[2] F. Rinderknecht, "A highly efficient energy converter for a hybrid vehicle concept—Focused on the linear generator of the next generation," in *Proc. 8th Int. Conf. Exhib. Ecolog. Vehicles Renew. Energies (EVER)*, Monte Carlo, Monaco, Mar. 2013, pp. 1–7.
[3] C. Yuting, H. Wei, S. Li, and R. Wang, "Review of free piston internal combustion engine," in *Proc. China Soc. Automot. Eng. Annu. Conf. Exhibit.*, Shanghai, China, Oct. 2016, pp. 325–329.
[4] X. Hou *et al.*, "Performance investigation of a free piston expander-linear generator for small scale organic Rankine cycle," *Appl. Therm. Eng.*, vol. 144, pp. 209–218, Nov. 2018.
[5] H. Xu, "Simulation and experimental research on compression ignition FPELG in-cylinder combustion," *Beijing Inst. Technol.*, pp. 36–51, 2015.
[6] Y. Wang, L. Chen, B. Jia, and A. P. Roskilly, "Experimental study of the operation characteristics of an air-driven free-piston linear expander," *Appl. Energy*, vol. 195, pp. 93–99, Jun. 2017.
[7] Y. Xu *et al.*, "Experimental investigation of a free piston expander-linear generator with different valve timings," *Appl. Therm. Eng.*, vol. 142, pp. 555–565, Sep. 2018.
[8] H. Zhang, F. Yu, G. Li, X. Hou, H. Liu, and Y. Tian, "Experimental study on characteristics of free-piston expander-linear generators driven by compressed air," *J. Agricult. Mech.*, vol. 48, no. 9, pp. 377–383, 2017.
[9] B. Jia, R. Mikalsen, A. Smallbone, and A. P. Roskilly, "A study and comparison of frictional losses in free-piston engine and crankshaft engines," *Appl. Therm. Eng.*, vol. 140, pp. 217–224, Jul. 2018.
[10] B. S. Preetham and L. Weiss, "Investigations of a new free piston expander engine cycle," *Energy*, vol. 106, pp. 535–545, Jul. 2016.
[11] C. Champagne and L. Weiss, "Performance analysis of a miniature free piston expander for waste heat energy harvesting," *Energy Convers. Manage.*, vol. 76, pp. 883–892, Dec. 2013.
[12] Y. Wu, Y. Wang, X. Zhen, S. Guan, and J. Wang, "Three-dimensional CFD (computational fluid dynamics) analysis of scavenging process in a two-stroke free-piston engine," *Energy*, vol. 68, pp. 167–173, Apr. 2014.
[13] Y. Gao, S. Shao, H. Zou, M. Tang, H. Xu, and C. Tian, "A fully floating system for a wave energy converter with direct-driven linear generator," *Energy*, vol. 95, pp. 99–109, Jan. 2016.
[14] C. Yuan, H. Ren, and J. Xu, "Experiment on the ignition performances of a free-piston diesel engine alternator," *Appl. Therm. Eng.*, vol. 134, pp. 537–545, Apr. 2018.
[15] J. Wang and D. Howe, "A linear permanent magnet generator for a free-piston energy converter," in *Proc. IEEE Int. Conf. Electr. Mach. Drives*, San Antonio, TX, USA, May 2005, pp. 1521–1528.
[16] J. Chen, Y. Liao, C. Zhang, and Z. Jiang, "Design and ananysis of a permanent magnet linear generator for a free-piston energy converter," in *Proc. 9th IEEE Conf. Ind. Electron. Appl. (ICIEA)*, Hangzhou, China, Jun. 2014, pp. 1719–1723.
[17] J. Wang, M. West, D. Howe, H. Z.-D. La Parra, and W. M. Arshad, "Design and experimental verification of a linear permanent magnet generator for a free-piston energy converter," *IEEE Trans. Energy Convers.*, vol. 22, no. 2, pp. 299–306, Jun. 2007.
[18] J. Lim, S.-K. Hong, and H.-K. Jung, "Design and analysis of 5 kw class tubular type linear generator for free-piston engine," *Int. J. Appl. Electromagn. Mech.*, vol. 35, no. 4, pp. 231–240, 2011.
[19] C. S. S. Hlaing and Z. H. Myint, "Design and analysis of tubular type linear generator for free piston engine," *Int. J. Sci. Eng. Technol. Res.*, vol. 3, no. 8, pp. 1326–1330, 2014.
[20] P. Zheng, C. Tong, J. Bai, B. Yu, Y. Sui, and W. Shi, "Electromagnetic design and control strategy of an axially magnetized permanent-magnet linear alternator for free-piston stirling engines," *IEEE Trans. Ind. Appl.*, vol. 48, no. 6, pp. 2230–2239, Nov./Dec. 2012.
[21] Y. Chen, H. Zhou, M. Tang, and Z. Li, "Analysis of free piston permanent magnet DC linear generators for internal combustion engines," *Small Special Mach.*, vol. 40, no. 5, pp. 19–22, 2012.
[22] F. Li, B. Xue, and P. Zheng, "A study on radial magnetization free-piston permanent magnet linear generator for electric vehicle," *Micromotors*, vol. 41, no. 2, pp. 22–24, 2008.
[23] P. Zheng, A. Chen, P. Thelin, W. M. Arshad, and C. Sadarangani, "Research on a tubular longitudinal flux PM linear generator used for free-piston energy converter," *IEEE Trans. Magn.*, vol. 43, no. 1, pp. 447–449, Jan. 2007.
[24] A. S. Jalal, N. J. Baker, and D. Wu, "Design of tubular moving magnet linear alternator for use with an external combustion—Free piston engine," in *Proc. 8th IET Int. Conf. Power Electron., Mach. Drives (PEMD)*, Glasgow, U.K., Apr. 2016, pp. 1–6.
[25] Y. Sui, Y. Liu, L. Cheng, J. Liu, and P. Zheng, "A tubular hybrid Halbach/axially-magnetized permanent-magnet linear machine," *AIP Adv.*, vol. 7, no. 5, 2017, Art. no. 056629.
[26] P. Zheng *et al.*, "Investigation of a 7-pole/6-slot Halbach-magnetized permanent-magnet linear alternator used for free-piston stirling engines," *J. Appl. Phys.*, vol. 111, no. 7, 2012, Art. no. 07E711.
[27] N. B. Hung and O. Lim, "A review of free-piston linear engines," *Appl. Energy*, vol. 178, pp. 78–97, Sep. 2016.
[28] M. R. Hanipah, R. Mikalsen, and A. P. Roskilly, "Recent commercial free-piston engine developments for automotive applications," *Appl. Therm. Eng.*, vol. 75, pp. 493–503, Jan. 2015.
[29] H. Zhou, "Analysis of free piston permanent magnet DC linear generator for internal combustion engine," *Tianjin Univ.*, pp. 9–10, 2011.

YONGMING XU was born in Shuozhou, Shanxi, China, in 1979. He received the Ph.D. degree in electrical machine and electrical apparatus from the Harbin University of Science and Technology, in 2008, where he has been a Professor with the School of Electrical and Electronic Engineering, since 2013. His research interests include design of special motor, numerical calculation of integrated physical field in motor, and research on local overheating and fluid field of super large transformer.

DIYUAN ZHAO was born in Shangqiu, Henan, China, in 1992. He received the M.S. degree in electrical machine and electrical apparatus from the Harbin University of Science and Technology, in 2019, where he is currently pursuing the master's degree with the School of Electrical and Electronic Engineering. His research interest includes design of special motor.

YAODONG WANG received the B.Sc., C.Eng., MIMechE, M.Sc., and Ph.D. degrees. He is currently a Senior Lecturer and a very Active Researcher working on sustainable, clean, and renewable energy at Newcastle University, U.K. He has 20 years of experience working on 24 research projects as a Principal Investigator (PI), a Co-Investigator (Co-I), and a Researcher (10 multi-disciplinary and multi-institutional), including the Miller cycle petrol and diesel engines, flameless oxidation to reduce NO_x emissions from gas turbine and power plant, biofuel petrol/diesel engine, biofuel trigeneration and cogeneration with energy storage, energy systems, such as biomass/coal thermal power stations, coal and biomass combustion and gasification, and organic Rankine cycle, renewable energy systems (wind solar, biomass, and water/hydropower), thermal energy management in processing industries, and building energy saving using passive and active methods.

MENGMENG AI was born in Harbin, Heilongjiang, China, in 1991. He received the M.S. degree in electrical machine and electrical apparatus from the Harbin University of Science and Technology, in 2017, where he is currently pursuing the Ph.D. degree with the School of Electrical and Electronic Engineering. Since 2017, he has been a Teaching Assistant with the School of Electrical and Electronic Engineering, Harbin University of Science and Technology. His research interests include optimal design of motor, numerical calculation of integrated physical field in motor, and research on local overheating and fluid field of super large transformer.